1D Nonlinear Acoustic Wave Equation In Heterogeneous Fluid

Renan A. Peres[1], Antônio M. F. Frasson[1], Carlos F. Loeffler[2], Fábio P. Piccoli[1], Julio T. A. Chacaltana[1]

[1] *Post-graduate Program in Environmental Engineering, Federal University of Espírito Santo*
Av. Fernando Ferrari, 514,Goiabeiras, 29075-910, Espírito Santo, Brazil
renan.peres@edu.ufes.br, antonio.frasson@ufes.br, fabio.p.piccoli@gmail.com, julio.chacaltana@ufes.br
[2] *Post-graduate Program in Mechanical Engineering, Federal University of Espírito Santo*
Av. Fernando Ferrari, 514,Goiabeiras, 29075-910, Espírito Santo, Brazil
carlosloeffler@bol.com.br

Abstract. In this work, the one-dimensional nonlinear equation of acoustic wave propagation in non-homogeneous fluid was developed using the physical laws of fluid mechanics and thermodynamics for a compressible fluid, including a source term for pressure wave generation. The solution of the 1D Acoustic Wave equation is performed in the time domain using the Petrov-Galerkin Finite Element Method (FEM), and the linear and parabolic approximation basis functions. In wave generation, two different types of pressure source term were implemented, the Ricker type (Chacaltana [1]; Picolli [2]) and the sinusoidal type. The boundary conditions of Neumann (natural reflection) and Reynolds [3] (Absorbing Boundary Condition - ABC) were also implemented and tested. To test the model, a Fortran code was written and a graphical interface in Octave was used to visualize and analyze the numerical results. Simulations were performed in a discrete domain of points representing the one-dimensional mesh. The non-uniform distribution of discrete points was obtained by the GMSH mesh generator. Numerical results were compared with those found in the literature. And, there was a good agreement between them.

Keywords: Non-linear Acoustic Wave equation; Non-homogeneous; Finite Element Method; Ricker wavelet.

1 Introduction

The study of Acoustic Waves propagation in non-homogeneous media has been the focus of study of many researchers due to the large number of applications of pressure waves (P-waves) and their impacts on technological development (Sheu & Fang [4]). The range of applications for acoustics is wide and ranges from the petroleum industry and communications sector to seismic exploration. As well as in the applications of high frequency waves found in the field of medicine, from medical ultrasound such as lithotripsy or HIFU therapy to ultrasonic cleaning or sonochemistry (Hoffelner & Kaltenbacher [5]). In this sense, it is of great interest to understand the transformations of the Acoustic Wave during its propagation and interaction with the environment as realistically as possible and in the most diverse scenarios. Thus, it is the object of this work to develop the non-linear equation to analyze the propagation of the P-wave in a non-homogeneous medium.

The Acoustic Waves propagation was studied by Kagawa [6], Campos-Pozuelo [7] and Hoffelner & Kaltenbacher [5] who used the plane wave approximation of Hamilton & Blackstock [8] and solved the non-linear form of the equation using a Finite Element Method - FEM. Other numerical methods used to solve the linear and nonlinear equation of the Acoustic Wave in the time domain are Finite Difference Method - FDM (Long [9]; Guimarães [10]) and Finite Volume Method - MVF (Pino [11]; Chacaltana [1]; Valente [12]).

In general, the classical Acoustic Wave equation is a linear and hyperbolic equation in the time domain involving second derivatives both in time and space, as used by Chacaltana [1] and Araujo [13] who performed pressure wave propagation (P-wave) in a layered homogeneous medium. The non-linear form involving only first derivatives can be found in Piccoli [2], who performed P-wave propagation in a non-homogeneous medium using FDM in the time domain. In this work, the one-dimensional nonlinear P-wave propagation equation for non-homogeneous medium is solved using FEM in the time domain. The mathematical deduction of the Acoustic Wave equation was obtained from the laws of conservation of mass and momentum and an equation of

state, considering a source term for pressure generation. The P-wave propagation model is manipulated and placed into second derivatives both in time and space.

In this work, Weighted Residuals Method (Petrov-Galerkin) and the linear and quadratic basis functions were used to solve the non-linear P-wave propagation equation by the FEM. The one-dimensional continuous domain was represented by discrete points and non-uniformly distributed, forming a mesh of n elements. The non-uniform distribution of points was obtained by the GMSH generator (v.4;11.1). At the domain boundaries, Neuman's reflexive boundary condition (natural) and the absorbing or non-reflective boundary condition - ABC as proposed by Reynolds (1978) were implemented. To generate the acoustic signal, two types of pressure sources were considered, Ricker-type wavelet (Piccoli [2]) and a monochromatic harmonic signal of the sinusoidal type. The numerical stability criterion was implemented as proposed by Oden & Fost [14].

Numerical tests are performed comparing the linear and non-linear model results for homogeneous and non-homogeneous media. Finally, a comparison between the results of the developed model and the experimental results is presented

2 Non-linear Acoustic Wave Equation for non-homogeneous medium

The pressure wave is a mechanical wave that is closely linked to the composition of the medium in which it propagates. The P-Wave equation for a compressible fluid medium is developed from the laws of fluid mechanics and thermodynamics. Following Chacaltana [1] and Piccoli [2], the equations representing the laws of conservation, mass and momentum, and thermodynamics for a compressible fluid and an isentropic process (constant entropy) can be written, respectively, in 1D, as:

$$\frac{d\rho}{dt}+\rho\frac{\partial u}{\partial x}=\dot{M} \tag{1}$$

$$\rho\frac{du}{dt}=-\frac{\partial p}{\partial x} \tag{2}$$

$$E=\rho c^2 \tag{3}$$

where c $\left[c^2=(\frac{\partial p}{\partial \rho})_s\right]$ is the P-wave velocity for an isentropic process. E $\left[E=\rho\frac{dp}{d\rho}\right]$ the fluid compressibility modulus. Thus, the equation of state, eq. (3), describes the compression and expansion of the medium (Lauterborn [15]). ρ is the specific mass, p the pressure, u the fluid velocity and $\dot{M}$ a mass source.

Using eq. (3), the definition of compressibility modulus and the Lagrangian derivative, eq. (1) and eq. (2) can be rewritten respectively as:

$$\frac{\rho}{E}(\frac{\partial p}{\partial t}+u\frac{\partial p}{\partial x})+\rho\frac{\partial u}{\partial x}=\dot{M} \tag{4}$$

$$\frac{\partial u}{\partial t}+u\frac{\partial u}{\partial x}=-\frac{1}{\rho}\frac{\partial p}{\partial x} \tag{5}$$

If the properties of the fluid are known, eq. (4) and eq. (5) represent a closed set of equations, for u and p.

Taking the partial derivative in time in eq. (4) and using eq. (5) we obtain the equation in second derivatives both in time and in space for the pressure.

$$\frac{\partial}{\partial t}(\frac{1}{E}\frac{\partial p}{\partial t})-\frac{\partial}{\partial x}(\frac{1}{\rho}\frac{\partial p}{\partial x})+\frac{\partial}{\partial t}(\frac{u}{E}\frac{\partial p}{\partial x})-\frac{\partial}{\partial x}(u\frac{\partial u}{\partial x})=\frac{P_f}{\rho} \tag{6}$$

Equations (5) and (6) form the non-linear model for P-wave propagation, where P_f is the pressure source term.

2.1 Initial and Boundary Conditions

The initial conditions for eq. (6) at time t_0 are:

$$p(x,t_0)=p_0 \tag{7}$$

$$\frac{\partial p(x,t_0)}{\partial t} = \dot{p}_0 \tag{8}$$

At the domain boundaries, the boundary conditions are the Dirichlet condition (essential) and the Neumman condition (natural), expressed respectively as:

$$p(x_c,t) = p_c(t) \tag{9}$$

$$\frac{\partial p(x_c,t)}{\partial x} = p_n(t) \tag{10}$$

2.2 Source term

The pressure sources used to generate the acoustic signal are the Ricker type, which consists of generating a pulse through the second derivative of Gaussian function; and the sinusoidal type to generate a monochromatic harmonic signal. The implemented Ricker wavelet is, (Piccoli [2]):

$$P_{f1}(t) = t_0 e^{(-0.25\pi f_c^2 t_0^2)} \tag{11}$$

where $t_0 = t - \frac{2\sqrt{\pi}}{f}$ and t is the time for the generated pulse, and f_c is the central frequency, defined in terms of the cutoff frequency f:

$$f_c = 3\sqrt{f} \tag{12}$$

For the generation of the harmonic signal, a sinusoidal type source was implemented:

$$P_{f2}(t) = A_0 \sin(-\omega t) \tag{13}$$

where A_0 is the initial amplitude, ω the angular frequency and t is the time. To smooth the beginning of the simulation, multiply eq. (19) by a function w described by the behavior of the hyperbolic tangent:

$$w(t) = \frac{1}{2}(1 + \tanh(\omega_e(t - T_{env}))) \tag{14}$$

Thus, we have the second source term defined as the second derivative of the product of (13) and (14):

$$P_f = \frac{\partial^2 (P_{f2} w)}{\partial t^2} \tag{15}$$

2.3 Stability Criterion

The numerical stability criterion follows the criterion presented by Oden & Fost (1973) for nonlinear hyperbolic equations:

$$\Delta t < \frac{\sqrt{2}h}{2c_{max}} \tag{16}$$

where h is the element size and c_{max} is the maximum wave speed.

3 Finite Element Method

The numerical solution of eq. (6) for the pressure is performed together with eq. (5) for the calculation of the velocity u. In eq. (5) the pressure gradient is assumed to be known. And, in eq. (6) both the velocity and its gradient are assumed to be known. Applying the FEM to eq. (5) to minimize the residue produced by the approximate solution multiplied by the weight function, w, we have:

$$<\frac{\partial u}{\partial t}, w> = <-\frac{1}{\rho}\frac{\partial p}{\partial x}, w> - <u\frac{\partial u}{\partial x}, w> \tag{17}$$

Performing the inner product for every one-dimensional domain, we have:

$$\int w\frac{\partial u}{\partial t}dx=-\int w\frac{1}{\rho}\frac{\partial p}{\partial x}dx-\int wu\frac{\partial u}{\partial x}dx \tag{18}$$

On the right side of eq. (18), the pressure gradient is considered known and the non-linearity that appears in the second term is linearized considering the velocity *u* known, both evaluated in the previous time "*n-1*".

$$\frac{\partial}{\partial t}\int w\,u\,dx=-\int\left(\frac{\partial p}{\partial x}\right)^{n-1}\frac{w}{\rho}dx-\int u^{n-1}w\frac{\partial u}{\partial x}dx \tag{19}$$

Using the Weighted Residuals Method (Petrov-Galerkin), the physical quantity of interest *u* can be assumed as the sum of its nodal values u_j multiplied by the approximation basis functions N_j, which are equal to the weight functions *w* (N_i), we have:

$$\frac{\partial}{\partial t}\int N_i\left(\sum_{i=1}^{Nn}u_jN_j\right)dx=-\int\left(\frac{\partial p}{\partial x}\right)^{n-1}\frac{N_i}{\rho}dx-\int u^{n-1}N_i\frac{\partial\left(\sum_{i=1}^{Nn}u_jN_j\right)}{\partial x}dx \tag{20}$$

where *Nn* is the number of nodes. Using finite differences in the time derivative, the discrete form of eq. (20) is.

$$\frac{\{u\}^n-\{u\}^{n-1}}{\Delta t}\int N_iN_j\,dx=-\int\left(\frac{\partial p}{\partial x}\right)^{n-1}\frac{N_i}{\rho}dx-\{u\}^{n-1}\int u^{n-1}N_i\frac{\partial N_j}{\partial x}dx \tag{21}$$

In matrix form, eq. (21) can then be written as:

$$\{u\}^n=([Re]-\{u\}^{n-1}[Md])\frac{\Delta t}{[M]}+\{u\}^{n-1} \tag{22}$$

where the matrix [*Md*] represents the non-linearity of the equation of motion.

Applying the same procedure to eq. (6), we obtain the matrix form for calculating the pressure, eq. (23):

$$\{p\}^{n+1}=\frac{\Delta t^2c^2\{P_f\}-\Delta t^2c^2[K]\{p\}^n-\Delta t([D]\{p\}^n-[D]\{p\}^{n-1})-\Delta t^2E[Kd]\{u\}^n+[M](2\{p\}^n-\{p\}^{n-1})}{[M]} \tag{23}$$

where the matrices [*D*] and [*Kd*] represent the non-linearity of the equation, that is, they depend on the induced velocity *u* calculated through eq. (22).

4 Results and Discussion

Case 1: Homogeneous medium: Linear and Non-Linear Solution

The case corresponds to a homogeneous aqueous medium with constant density ρ (1000 Kg/m^3) and speed of sound c (1500 m/s). The linear solution for pressure and velocity is obtained by setting the matrices [Md], [D] and [Kd] equal to zero. The domain of 15000 m in length is represented by 1500 second-order elements. The time interval is 10^{-3} s., which satisfies the stability criterion of Oden & Fost [14]. The sinusoidal source, placed in the center of the domain, has a frequency of 1 Hz. ABC boundary conditions were used at the borders. The simulation time was 600s (Figure 1), both for the linear and non-linear models.

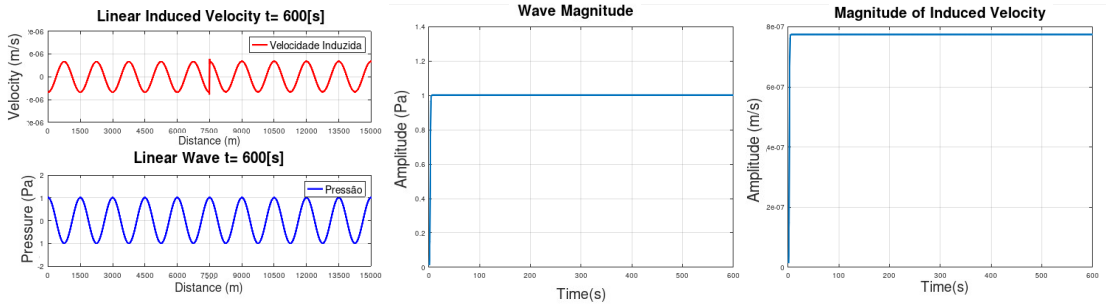

Figure 1. Linear pressure magnitude and induced velocity in Homogeneous Medium

After the simulation time of 17 sec., the pressure amplitude of the linear model reached a constant value of

0.999902 Pa. The velocity magnitude reached a constant value of 7.74464×10^{-7}m/s after the simulation time of 11 sec. The nonlinear model produced the same results for pressure and velocity. Regarding the results of the linear model, no significant difference was found between pressures and velocities, perhaps because the magnitude of the velocity is very small (~1μm/s). Table 1 presents the results of this first case.

Table 1. Results of pressure and velocity magnitude of linear and non-linear models for a homogeneous medium

Linear	Pressure	Fluid Velocity	**Non-Linear**	Pressure	Fluid Velocity
10s	1.001244Pa	7.74466×10^{-7}m/s	10s	1.001244Pa	7.74466×10^{-7}m/s
11s	1.001159Pa	7.74464×10^{-7}m/s	11s	1.001159Pa	7.74464×10^{-7}m/s
17s	0.999902Pa	7.74464×10^{-7}m/s	17s	0.999902Pa	7.74464×10^{-7}m/s
600s	0.999902Pa	7.74464×10^{-7}m/s	600s	0.999902Pa	7.74459×10^{-7}m/s

Case 2: Heterogeneous medium: Linear and Non-Linear Solution

For heterogeneous medium, a 15 km domain with 2080 non-uniform second order elements was used. The source is a Ricker type with a cut-off frequency of 1 Hz. The domain was divided into three layers, the specification of each layer is shown in Table 2. At the borders, the absorbing condition (Air layer) and the reflective condition (Rock layer) were used. The time interval used was 2×10^{-4} s.

Table 2. Specifications of the 3 Layers of the Heterogeneous Domain

	Air layer (0 to 5km)	**Water layer** (5km to 10km)	**Rock layer** (10km to 15km)
Sound Speed	344m/s	1500m/s	5000m/s
Density	1Kg/m^3	1000Kg/m^3	2500m/s

At each interface between the layers (5km / 10km) the P-wave is transmitted and reflected. Figure 2 shows this interaction from 3 s to 7.5 s.

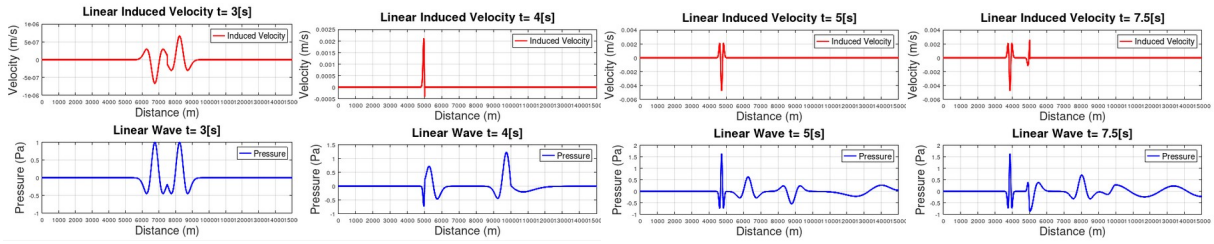

Figure 2. Pressure and velocity magnitude of the linear model for heterogeneous media

During propagation, the interaction of the wave with the change of medium takes place in the form of reflection. Thus, the energy of the incident wave is divided into one that is carried by the reflected wave and one that is carried by the transmitted wave. After the reflection of the wave at the boundary of the domain (rock layer) and back to the water layer, the amplitude of the wave is smaller than the initial amplitude. In the water layer, the initial amplitude of the wave propagating towards the rock layer (at 3s) was 0.99996Pa, while an amplitude of 0.71004Pa was recorded on its return (at 7.5s). The speed also varied, going from 6.6677×10^{-7}m/s to 4.7345×10^{-7}m/s when returning to the water layer. The wave propagating towards the air layer reached an amplitude of 1.6268Pa after reflection at the water/air interface (in 7.5s). As can be seen in Table 3, the linear and non-linear model results are essentially the same.

Table 3. Pressure magnitude and induced velocity from second case

Linear	Pressure	Velocity	**Non-Linear**	Pressure	Velocity
Right Wave - 3s	0.99999Pa	$6.6677x10^{-7}$m/s	Right Wave - 3s	0.99996Pa	$6.6652x10^{-7}$m/s
Right Wave - 7.5s	0.71004Pa	$4.7345x10^{-7}$m/s	Right Wave - 7.5s	0.70999Pa	$4.7348x10^{-7}$m/s
Left Wave - 3s	1Pa	$6.6666x10^{-7}$m/s	Left Wave - 3s	1Pa	$6.6666x10^{-7}$m/s
Left Wave - 7.5s	1.6268Pa	$4.7401x10^{-3}$m/s	Left Wave - 7.5s	1.6251Pa	$4.7352x10^{-3}$m/s

Case 3: Linear and Non-Linear Solution for high sound pressure level

For the latter case, a source with a high sound pressure level (SPL) was considered according to the scenario analyzed numerically and experimentally by Zhou [16]. The objective was to investigate the linear and non-linear behavior for high pressure sources and compare the numerical results with those of Zhou [16].

In this scenario, a 160 dB acoustic source in mid-air (ρ~1 Kg/m^3 and c=344 m/s) was used to generate an acoustic wave of 1000 Hz. At a distance of half a wavelength from the source (x = 0.17m) a receiver was placed to analyze the passage of the wave. Considering that 160 dB equals approximately 10000 W/m^2, a pressure variation around 2600 Pa was used as the amplitude of the pressure source. A 2 m long mesh is used and the discrete form is represented by 200 second-order elements. The time interval used was $1x10^{-6}$s. Due to the use of an attenuation function of 5 wave periods at the beginning of the simulation, the first 5 ms were disregarded and only the results of the following 3.5 ms were analyzed.

The velocity results of the linear and non-linear models are in good agreement with those of Zhou [16], reaching more than 6m/s at pressure peaks of 160dB at a distance of half a wavelength from the source (Figure 3), as reported by Zhou [16] when commenting that "[...] the peak velocity of the particle increases with the SPL, and when this level reaches 160 dB, the peak velocity of a 2μm particle can exceed 6 m/s ".

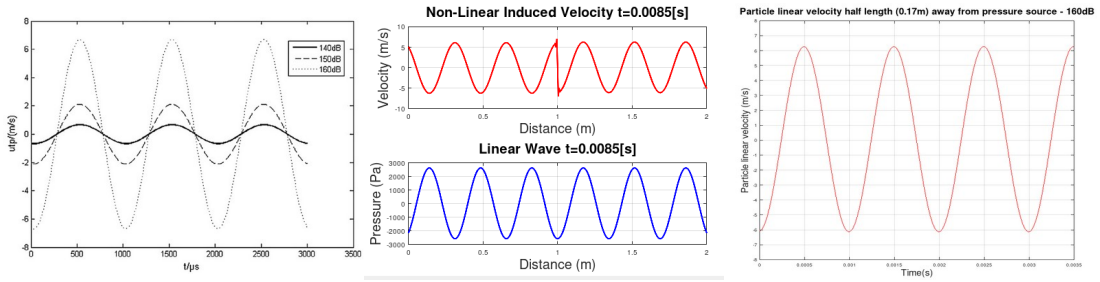

Figure 3. Zhou's results, linear pressure magnitude and particle velocity from a 160dB pressure source

Table 4. Comparison between linear and non-linear particle velocity and pressure at x=0.17m and t=3.5ms

160dB source	**Linear**	**Non-Linear**
Particle Velocity	6,264 m/s	6.239 m/s
Pressure	2600.81 Pa	2 617.35 Pa

Particle velocities in the linear and non-linear models also showed good agreement with each other, as shown in Table 4. For a pressure source of 160 dB, a greater difference was noted between the particle velocities in the linear and non-linear models in compared to the previous cases, indicating that the velocity of the non-linear model may become more significant as the source intensity increases. However, this difference was still small (~0.4%), indicating that despite being a relatively intense acoustic source for humans, it can be considered small for the environment, since the non-linear effects did not act significantly.

5 Conclusion

The results found by the model are in agreement with those reported in the literature in experimental works, on the magnitude of the velocity induced by sound. Taylor [17] reports induced velocities of the order of 10^{-5}m/s for low frequency Acoustic Waves, and Dall'Osto [18] reports induced velocities of the order of 10^{-6}m/s recorded during the propagation of a 100ms acoustic pulse in shallow waters, through the superimposition of four tones of continuous wave, centered in 1025, 2050, 3075 and 3950 Hz. Despite the results of the linear and non-linear models being very close in the tests carried out in this work, the non-linear model is promising. Case 3 shows that an increase in the pressure source leads to a greater difference between the results of the linear and non-linear model, whose difference is of the order of 10^{-2}m/s for induced velocity of the order of 10^{0} m/s.

Acknowledgements. The authors would like to thank the *Fundação de Amparo à Pesquisa do Estado do Espírito Santo* (FAPES) for financial support in carrying out this research.

Authorship statement. The authors are responsible for the authorship of this work and for the preparation of the material included here as part of this article.

References

[1] Chacaltana, J. T. A. et al. Volumes Finitos não Estruturados voltado à Propagação de Ondas Acústicas em Meios Heterogêneos. In: PROCEEDINGS OF THE XLI IBERO-LATIN-AMERICAN CONGRESS ON COMPUTATIONAL METHODS IN ENGINEERING, Rio de Janeiro. Anais… Rio de Janeiro, CILAMCE, 2015.
[2] Piccoli, F. P. et al. Nonlinear Acoustic Wave Propagation in Stratified Media. In: PROCEEDINGS OF THE XLI IBERO-LATIN-AMERICAN CONGRESS ON COMPUTATIONAL METHODS IN ENGINEERING, 41, 2020, Foz de Iguaçu. Anais… Foz de Iguaçu, CILAMCE, 2020.
[3] Reynolds, A. C. Boundary conditions for the numerical solution of wave propagation problems. Geophysics, v. 43, n. 6, p. 1099-1110, 1978.
[4] Sheu, T. W. H.; Fang, C. C. A high resolution finite element analysis for nonlinear acoustic wave propagation. Journal of Computational Acoustics, v. 2, n. 1, p. 29-51, 1994.
[5] Hoffelner, J.; Kaltenbacher, M. Finite Element Simulation of Nonlinear Wave Propagation in Thermoviscous Fluids Including Dissipation. IEEE Transactions on Ultrasonics, Ferroelectrics, and Frequency Control, v. 48, n. 3, P. 779-786, 2001.
[6] Kagawa, Y. et al. Finite Element Simulation of Non-Linear Sound Wave propagation. Journal of Sound and Vibration, v. 154, n. 1, p. 125-145, 1992.
[7] Campos-Pozuelo, C. et al. Finite-element analysis of the nonlinear propagation of high-intensity acoustic waves. Journal of Acoustic Society of America, v. 106, n. 1, p. 92-101, 1999.
[8] Hamilton, M. F.; Blackstock, D. T. On the coefficient of nonlinearity in nonlinear acoustics. Journal of Acoustic Society of America, v. 86, n. 1, p. 74-77, 1987.
[9] Long, G.; Zhao, Y.; Zou, J. A temporal fourth-order scheme for the first-order acoustic wave equations. Geophysics J. Int., v. 194, p. 1473 – 1485, 2013.
[10] Guimarães, R. F. Modelador de propagação de onda acústica 2D por diferenças finitas no domínio do tempo em CUDA. 68f. Dissertação (Mestrado), Programa de Pós-Graduação em Ciência e Engenharia de Petróleo, Universidade Federal do Rio Grande do Norte, Natal, 2018.
[11] Pino, S. D. et al. 3D Finite Volume simulation of acoustic waves in the earth atmosphere. Computers & Fluids, v. 38, p. 765–777, 2009.
[12] Valente, A. et al. 3D OcTree Finite-volume method for acoustic wave simulation. In: PROCEEDINGS OF THE XLI IBERO-LATIN-AMERICAN CONGRESS ON COMPUTATIONAL METHODS IN ENGINEERING, 2015, Rio de Janeiro. Anais… Rio de Janeiro, CILAMCE, 2015.
[13] Araujo, L. et al. Acoustic wave propagation in non-homogeneous media. In: PROCEEDINGS OF THE XLI IBERO-LATIN-AMERICAN CONGRESS ON COMPUTATIONAL METHODS IN ENGINEERING, 41, 2020, Foz de Iguaçu. Anais… Foz de Iguaçu, CILAMCE, 2020.
[14] Oden, J. T.; Fost, R. B. convergence, accuracy and stability of finite element approximations of a class of non-linear hyperbolic equations. International Journal for Numerical Methods in Engineering, v. 6, p. 357-365, 1973.
[15] Lauterborn, et al. Nonlinear Acoustic in Fluids. In: Physical and Nonlinear Acoustic. Springer Handbook of Acoustics, part. B, p. 257-297, 2007.
[16] Zhou, D. et al. Numerical calculation of particle movement in sound wave fields and experimental verification through high-speed photography. Applied Energy, 2016. http://dx.doi.org/10.1016/j.apenergy.2016.02.006
[17]Taylor, K. J. Absolute measurement of acoustic particle velocity. J. Acoust. Soc. Am., v. 59, n. 3, 1976
[18]Dall'Osto, D. R. et al. Measurement of acoustic particle motion in shallow water and its application to geoacoustic inversion. J. Acoust. Soc. Am, v. 139 ,n.1, 2016.